Desalination and Water Treatment
www.deswater.com

doi: 10.5004/dwt.2018.22816

126 (2018) 181–195
September

Single and competitive adsorptive removal of lead, cadmium, and mercury using zeolite adsorbent prepared from industrial aluminum waste

Ruth Sánchez-Hernández[a], Isabel Padilla[a], Sol López-Andrés[b], Aurora López-Delgado[a,*]

[a]*National Centre for Metallurgical Research, CSIC, Avda. Gregorio del Amo 8, Madrid, 28040, Spain, Tel. +34915538900; emails: alopezdelgado@cenim.csic.es (A. López-Delgado), ruthsh@cenim.csic.es (R. Sánchez-Hernández), isapadilla@cenim.csic.es (I. Padilla)*
[b]*Department of Mineralogy and Petrology, Faculty of Geology, University Complutense of Madrid, C/José Antonio Nováis 12, Madrid, 28040, Spain, email: antares@ucm.es (S. López-Andrés)*

Received 14 February 2018; Accepted 17 July 2018

ABSTRACT

The removal of Pb^{2+}, Cd^{2+}, and Hg^{2+}, which act as endocrine disruptors, from aqueous solutions was performed using a NaP1-type zeolite synthesized from a hazardous aluminum waste. The effects of parameters such as pH, contact time, adsorbent dose, initial cation concentration, and coexisting cations on the adsorption efficiency and capacity of the adsorbent were evaluated. Single-cation adsorption was found to be a fast process well described by the pseudo-second-order kinetic model. Equilibrium was reached in the first 15 min achieving high removal efficiencies: 98.9%, 93.3%, and 99.3% for Pb^{2+}, Cd^{2+}, and Hg^{2+}, respectively. The removal of the metal cations could occur via a homogeneous and physical adsorption process that was satisfactorily described by the Sips isotherm. The maximum adsorption capacities, obtained from the Sips isotherm model, were 245.75, 4.43, and 0.22 mg/g for Pb^{2+}, Cd^{2+}, and Hg^{2+}, respectively. In multi-cation adsorption, the zeolite presented the greatest affinity for Pb^{2+} (due to its smallest cationic size) compared with Cd^{2+} and Hg^{2+}. The Pb^{2+} removal efficiency remained practically constant in presence of Hg^{2+} and Cd^{2+}, reaching efficiencies near 100% at very low contact times (<5 min). Thus, this zeolite could become an alternative adsorbent to eliminate heavy metals from waters. A synergic effect on the environmental protection could be achieved: the end-of-waste condition of a hazardous waste as well as the water decontamination.

Keywords: Heavy metal; Endocrine disruptor; NaP1 zeolite; Adsorption kinetic; Equilibrium isotherm; Competitive adsorption; Water treatment

1. Introduction

Great efforts are being made to achieve the prevention and reduction of environmental concerns, such as water pollution, associated with the rapid global industrialization. Water pollution represents a threat to the aquatic organisms and to the health of human beings. Adequate identification and appropriate management are essential to control anthropogenic emissions of contaminants into waters. Among the most common pollutants present in aquatic media, heavy metals such as mercury, lead, and cadmium are considered endocrine disruptors due to their bioaccumulation in organisms causing serious health disorders, among others in the endocrine, nervous, and immune systems. Mercury is released principally from different activities, such as battery, thermometer and chlor-alkali production, paint and color industry, coal combustion, and waste incineration [1,2]. Anthropogenic sources such as gasoline and water distribution systems such as lead-containing pipes contribute to the release of lead [1]. Cadmium is released to industrial effluents from the steel electroplating and nickel–cadmium batteries manufacture [3]. The Directive 2013/39/EU concerning the priority substances in the field of water establishes

* Corresponding author.

maximum allowable concentrations in inland surface waters of 0.07, 14, and 0.45–1.5 μg/L for mercury, lead, and cadmium (depending on the hardness of the water) [4].

Developing more cost-effective wastewater treatment techniques by using low-cost sorbents and/or easily handled materials contributes to the environmental sustainability. Various technologies, such as filtration, electrochemical treatment, chemical precipitation, adsorption, ion-exchange, etc., have been developed for treatment of heavy metal-containing wastewaters. Although chemical precipitation is widely used, it usually requires large amounts of chemicals leading to secondary sludge production that needs to be treated, thus increasing process costs and environmental impacts [5]. On the contrary, adsorption represents a simple, efficient, and relatively economic technique for the removal of different pollutants from waters. It offers a very versatile design and allows for the use of a wide range of sorbents such as zeolites.

Zeolites are porous crystalline solids composed of tetrahedral TO_4 units (T = Si, Al, Ge, etc.) forming a three-dimensional framework with cages, channels, and cavities. These materials, formed in nature or synthetically obtained from diverse sources, are widely employed for the removal of numerous substances from aqueous media due to their excellent porosity and cation-exchange capacity (CEC).

In the last few decades, the use of waste-based sorbents for the removal of heavy metals from aqueous solutions has been widely investigated. For example, Apiratikul and Pavasant [6] studied the removal of Cu^{2+}, Cd^{2+}, and Pb^{2+} from aqueous solutions at pH 5 by using zeolite X from fly ash with a CEC of ~1.4 meq/g. Asencios and Sun-Kou [7] prepared scrap-based alumina to eliminate Pb^{2+}, Zn^{2+}, and Cd^{2+} from aqueous solutions at pH 3–5 reaching adsorption capacities of 13.1, 7.4, and 8.2 mg/g, respectively. Zhou et al. [8] investigated the adsorption of Pb^{2+} and Zn^{2+} using a biosorbent extracted from waste activate sludge. These authors reported high experimental adsorption capacities (451 and 267 mg/g for Pb^{2+} and Zn^{2+}, respectively) at pH 6 and 25°C after 30 min.

The investigation on other type of waste-based materials could lead to alternative sorbents. For example, industrial waste from aluminum metallurgy, due to their chemical and mineralogical composition, could be used to obtain zeolites with appropriate sorption properties.

In this sense, a hazardous aluminum waste (hereinafter, Al-waste) was recently used for the synthesis of high-CEC zeolites, which could be used as sorbents. This Al-waste is derived from aluminum slag milling processes, and it is considered as hazardous, especially, in contact with humidity due to its environmental risks [9,10]. The use of Al-waste in the synthesis of zeolites can contribute to minimize the waste generation [9,11], according to the end-of-waste criteria [12].

Zeolites such as NaP1 ($Na_6Al_6Si_{10}O_{32}{\cdot}12H_2O$) obtained from this Al-waste presented high CEC values ranged between 2.25 and 2.73 meq/g [9,11] compared with other zeolites reported in the literature [13–16]. NaP1 consists of a three-dimensional channel system with pore sizes ranged between 4.5 × 3.1 and 4.8 × 2.8 Å (according to the International Zeolite Association, IZA). This zeolite has two important characteristics: a good molecular sieve and a high CEC that make it a good candidate for the wastewater treatment.

To the best of our knowledge, there are no earlier works focusing on the removal of heavy metals using NaP1 obtained from Al-waste (hereinafter, Al-waste-NaP1). This work deals with the feasibility of using Al-waste-NaP1 for the treatment of aqueous solutions containing Pb^{2+}, Cd^{2+}, and Hg^{2+}. The effects of parameters, including pH, adsorbent dose, contact time, initial cation concentration, and coexisting cations in the solution medium were evaluated. Different kinetic and isotherm models were applied to study the behavior of Al-waste-NaP1 during adsorption. In addition, its morphological, structural, and chemical properties were analyzed before and after the competitive adsorption of Pb^{2+}, Cd^{2+}, and Hg^{2+} to better understand the studied adsorption system.

2. Materials and methods

2.1. Adsorbent

The zeolite used in this work was synthesized from a hazardous aluminum waste (Al-waste) at 120°C for 6 h by a sustainable synthesis process according to our previous study [11]. It allows the complete transformation of Al-waste into a NaP1-type zeolite (Al-waste-NaP1).

2.2. Adsorbates

All chemicals used for the adsorption tests were analytical reagents of high purity. Aqueous solutions containing the cations were prepared with deionized water with a resistivity of 18.2 MΩ·cm. A stock solution (1,000 mg/L) of the Pb^{2+} cation was prepared by dissolving the required amount of pure lead metal (99.9% purity, Merck) firstly in HNO_3 and then in ultrapure water. A stock solution (1,000 mg/L) of the Cd^{2+} cation was prepared by dissolving a cadmium chloride salt (99.995% purity, Sigma-Aldrich) in ultrapure water containing 4%–5% HNO_3 (69%, Panreac). A commercial standard solution (Hg 1000 mg/L in 2%–5% HNO_3, Panreac) was used to perform the adsorption experiments of the Hg^{2+} cation. To avoid the precipitation of the metal cations, in particular Pb^{2+}, which tends to form $PbCl_2$ in contact with HCl, the pH values required for the adsorption experiments were adjusted by adding dilute NaOH (98%–100.5% purity, Panreac) or HNO_3 (69%, Panreac) aqueous solutions.

2.3. Adsorption procedure

Batch experiments of Pb^{2+}, Cd^{2+}, and Hg^{2+} adsorption were carried out at room temperature (25°C ± 2°C). The required amounts of zeolite were placed in 150 mL Erlenmeyer flasks containing 100 mL of metal cation solution and stirred at 125 rpm using an orbital and horizontal shaker (Selecta, Rotabit). The influence of adsorption parameters, such as pH, contact time, adsorbent dose, and initial concentration, on the removal of each metal cation (single adsorption) was evaluated. For the competitive adsorption experiments, the effect of the coexisting metal cations on the removal ability of the zeolite was also studied.

2.3.1. Effect of pH

In order to determine the optimal operating conditions for the adsorption process, the effect of pH on the metal

cations and on the adsorbent was studied. The speciation of lead, cadmium, and mercury in aqueous medium was evaluated using fixed initial concentrations (20 mg/L for Pb^{2+} and Cd^{2+}, and 0.2 mg/L for Hg^{2+}) in a pH range of 2–12. The influence of pH on the crystalline and morphological properties of the zeolite was studied. For this, a fixed zeolite mass (5 g) was placing in contact with a fixed aqueous solution volume (250 mL) at different pH values. Unlike the Pb^{2+} and Cd^{2+} cations, the Hg^{2+} cation is more strongly influenced by the solution pH. Therefore, the effect of pH on the Hg^{2+} adsorption was evaluated at pH 2–6 using an initial Hg^{2+} concentration of 0.2 mg/L and an adsorbent dose of 10 g/L to select the best conditions. Further adsorption tests for all the metal cations were performed under the pH selected as optimal.

2.3.2. Effect of contact time

The effect of the contact time on the adsorption efficiency of Al-waste-NaP1 was evaluated from 1 to 120 min using the initial concentrations studied (20 mg/L for Pb^{2+} and for Cd^{2+}, and 0.2 mg/L for Hg^{2+}) and the optimal adsorbent dose for each cation at pH 4.5. The adsorption kinetics of all the cations were also evaluated applying the pseudo-first [17] and pseudo-second-order [18] models, as well as the intra-particle diffusion model [19].

Unlike the pseudo-second and pseudo-first-order kinetic models, the intra-particle diffusion model can provide information about the reaction pathways and adsorption mechanisms, predicting the rate-controlling step. The internal surface and pore diffusion of an adsorbate inside an adsorbent may represent the rate-limiting steps. When this model represents a straight line that passes through the origin, the adsorption process is mainly governed by intra-particle diffusion; on the contrary, a multi-step adsorption process is given by multiple linear regions [20].

2.3.3. Effect of adsorbent dose

The effect of the zeolite dose (0.125–10 g/L) on the removal efficiency and adsorption capacity was studied using fixed initial concentrations (20 mg/L for Pb^{2+} and Cd^{2+}, and 0.2 mg/L for Hg^{2+}) at pH 4.5 for 30 min to ensure sufficient equilibrium time.

2.3.4. Effect of initial concentration

The adsorption equilibrium experiments were developed at pH 4.5, using the optimal adsorbent dose and contact time: 0.5 g/L and 30 min for Pb^{2+}, 5 g/L and 30 min for Cd^{2+}, and 5 g/L and 60 min for Hg^{2+}. The effect of the initial concentration of each metal cation on the adsorption ability of the adsorbent was evaluated using the following isotherm models: Langmuir [21], Freundlich [22], Dubinin–Radushkevich [23], Redlich–Peterson [24], Toth [25], and Sips [26], which are widely used for the removal of different pollutants from water.

The isotherms were evaluated for different initial concentrations of the metal cations: 5–100 mg/L for Pb^{2+}, 1–40 mg/L for Cd^{2+}, and 0.02–1.5 mg/L for Hg^{2+}.

2.3.5. Effect of competitive adsorption of Pb^{2+}, Cd^{2+}, and Hg^{2+}

The competitive adsorption of Pb^{2+}, Cd^{2+}, and Hg^{2+} on the zeolite was studied in the adsorbent dose range of 2–10 g/L at pH 4.5, for contact times ranged from 1 to 30 min under ambient conditions (25 ± 2°C).

Table 1 summarizes all conditions studied in the single- and multi-cation adsorption experiments using Al-waste-NaP1.

After reaching adsorption equilibrium, all the solutions were collected by filtration. The adsorption tests were performed in duplicate, representing the error bars and average values. The removal efficiency of the zeolite (expressed in %) and the amounts of Pb^{2+}, Cd^{2+}, and Hg^{2+} adsorbed on the zeolite at any time (q_t, expressed in mg/g) and at equilibrium (q_e, in mg/g) were calculated according to the next equations:

$$\text{Removal}(\%) = \left(\frac{C_o - C_t}{C_o}\right) \times 100 \quad (1)$$

$$q_t = \frac{(C_o - C_t)}{m} \times V \quad (2)$$

$$q_e = \frac{(C_o - C_t)}{m} \times V \quad (3)$$

where C_o (mg/L) is the initial concentration of metal cation, C_t and C_e (mg/L) are the cation concentrations at contact time t

Table 1
Conditions studied in the single- and multi-cation adsorption experiments using Al-waste-NaP1

Conditions	pH	Adsorbent dose (g/L)	Time (min)	Initial concentration (mg/L)
Lead (Pb^{2+}) adsorption				
Contact time	4.5	0.5	1–120	20
Adsorbent dose		0.125–1	30	20
Initial concentration		0.5	30	5–100
Cadmium (Cd^{2+}) adsorption				
Contact time	4.5	5	1–120	20
Adsorbent dose		1–10	30	20
Initial concentration		5	30	1–40
Mercury (Hg^{2+}) adsorption				
pH	2–6	10	1–120	0.2
Contact time	4.5	5	1–120	0.2
Adsorbent dose		1–10	30	0.2
Initial concentration		5	60	0.02–1.5
Multi-cation adsorption: Pb^{2+}, Cd^{2+}, and Hg^{2+}				
Conditions	4.5	2 and 10	1–30	20 (for Pb^{2+} and Cd^{2+}); 0.2 (for Hg^{2+})

and at equilibrium, respectively, m (g) is the mass of zeolite, and V (L) the volume of metal cation solution.

2.4. Kinetic and isotherm modeling

A non-linear optimization method using Microsoft Excel Solver was applied for the evaluation of the goodness of fit of the different models. All the parameters and constants of the studied kinetic and isotherm models were determined by maximizing the coefficient of determination (R^2):

$$R^2 = 1 - \left[\frac{\sum_{i=1}^{n} \left(q_{i,\text{exp}} - q_{i,\text{model}} \right)^2}{\sum_{i=1}^{n} \left(q_{i,\text{exp}} - q_{l,\text{exp}} \right)^2} \right] \quad (4)$$

where n is the number of experimental values in a dataset, and $q_{i,\text{exp}}$ and $q_{i,\text{model}}$ are the experimental and calculated adsorption capacities.

2.5. Characterization techniques

Zeta potential (ζ-potential) was determined by the electrophoretic mobility of zeolite particles in aqueous solutions at different pH (ZetaSizer Nano, Malvern). The samples were prepared using 0.05 g of zeolite per 100 mL of aqueous solution. Zeolite suspensions were stirred in an ultrasonic bath and kept in contact for a long time (24 h) to achieve equilibrium conditions before the ζ-potential measurements. Absolute ζ-potential values > 20 mV indicate electrically stable suspensions [27,28]. Point of zero charge (PZC) analysis was determined by preparing zeolite aqueous suspensions adjusted at different pH values using dilute HNO_3 or NaOH. The suspensions were agitated for 24 h until the equilibrium pH was reached. Mineralogical composition of the zeolite was evaluated by X-ray diffraction (XRD) (Bruker, D8 Advance) using the ICDD PDF reference pattern database. Crystallite sizes of the zeolite in contact with aqueous solutions at different pH were determined using the Scherrer [29] equation. The morphological characterization of the zeolite after the multi-cation removal was performed using scanning electron microscope (SEM), in a Hitachi S4800 microscope. The immobilization of all the metal cations on the adsorbent was characterized using Fourier-transform infrared (FTIR) spectroscopy (Bruker IFS 66Vs). Additionally, energy dispersive micro X-ray fluorescence (μ-XRF) analysis (Fischer, Fischerscope XUV 773) was performed to compare the initial chemical composition of the zeolite with that one after the multi-cation adsorption.

The variation of the concentrations of the Pb^{2+} and Cd^{2+} cations was determined by using ICP-OES (Perkin Elmer, Optima 3300 DV). The concentration of the Hg^{2+} cation was obtained using cold vapor atomic absorption spectrometry (PS Analytical, 10.025 Millennium Merlin) at wavelength of 235 nm. The variation of the solution pH was controlled using a pH meter (Crison, MM41). The chemical equilibrium diagrams of Pb^{2+}, Cd^{2+}, and Hg^{2+} in aqueous solution were obtained using the software MEDUSA (Make Equilibrium Diagrams Using Sophisticated Algorithms) for the following initial concentrations: 20 ppm for Pb^{2+}, 20 ppm for Cd^{2+}, and 0.2 ppm for Hg^{2+}.

3. Results and discussion

3.1. Textural and surface characterization of the zeolite

The main textural properties, type of isotherm, pore size distribution, and CEC of the zeolite are shown in Table S1 and Fig. S1. The zeolite shows a high CEC although the value of its BET-specific surface area is low. This value was almost identical to the external area because of its mesoporosity. The characterization of the zeolite surface was analyzed by determining its ζ-potential and PZC (Fig. S2). The ζ-potential, which is related to the external surface charge of the zeolite [30], revealed that it is positively charged at pH 3–5 and negatively charged above pH ~6. The point where the ζ-potential is zero, called the isoelectric point (IEP), represents the point where the system is least stable. The IEP of the zeolite was reached at approximately pH 5.8. Although the reviewed literature reports many zeolites with IEP obtained at lower pH conditions [31], there are some exceptions including IEP values close to our results. For example, Arancibia-Miranda et al. [32] reported a similar ζ-potential curve which reached the IEP at pH = 6, for a natural zeolite that exhibited good affinity for the uptake of heavy metals such as Pb^{2+} at pH 3–6. The surface charge of zeolites could depend on their Si/Al ratio. Previous works have stated that zeolites with high Al-content (i.e., Si/Al ratios < 2) can present IEP values at neutral pH conditions [30]. This behavior could be associated to materials with particle surfaces dominated mainly by aluminol groups. Compounds such as aluminas show similar behavior, presenting positive ζ-potential values at acid conditions (e.g., ζ-potential close to 30 mV at pH ~4.5, according to [33]). The PZC of Al-waste-NaP1 was reached at approximately pH 10.0. The PZC is associated with the total surface charge (i.e., the external and internal surface charge) and indicates that the surface charge density of the zeolite is zero at pH 10.0. As the difference between PZC and IEP is higher than one (i.e., $pH_{PZC} - pH_{IEP} > 1$), the external surface of Al-waste-NaP1 could be more negatively charged than the internal one [34].

3.2. Effect of pH

Among all the influencing parameters, pH can affect the solubility and speciation of metal ions, and it can also affect the properties of sorbent materials [35]. Several works in the literature have shown that the pH plays a key role, affecting the sorption of diverse contaminants such as heavy metals by different sorbents, including zeolites [15,32,36,37]. In this work, the effect of pH on the concentration of the studied metal cations, referred to their initial concentration (20 mg/L for Pb^{2+} and Cd^{2+}, and 0.2 mg/L for Hg^{2+}), was evaluated, as shown Fig. 1(a). As the pH increased up to pH 8 for Pb^{2+} and Hg^{2+}, and up to pH 10 for Cd^{2+} approximately, the stability of the cations in the aqueous solution decreased due to their hydrolysis. The chemical equilibrium diagrams of the Pb^{2+}, Cd^{2+}, and Hg^{2+} cations in aqueous solution were determined for the same initial concentrations (Fig. S3). The Pb^{2+} cation is stable in aqueous medium until pH ~6, partially hydrolyzing to form $PbOH^+$ and $Pb(OH)_2$ as pH increases. The Cd^{2+} cation is very stable up to around pH 9. As the basicity of the aqueous medium increases, the formation of cadmium species such as $CdOH^+$, $Cd(OH)_2$, and $Cd(OH)_3^-$ is favored. On the contrary, the Hg^{2+} cation is stable in very acid medium

(until pH ~4). An increase of the pH leads to the hydrolysis of mercury to form $HgOH^+$ and subsequently $Hg(OH)_2$, coexisting these mercury species at pH < 6. Thus, the formation of soluble and/or precipitated species of each metal strongly depends on the solution pH used to remove them.

As the removal of Hg^{2+} is highly dependent on the solution pH, the effect of this parameter was studied in a pH range of 2–6 (Fig. 1(b)) to select the optimal pH conditions for the single- and multi-cation uptake. The removal ability of Al-waste-NaP1 was found to be practically unchanged at higher pH than 2, in particular at pH ranged between 4 and 6. The adsorption efficiency of the zeolite decreased at low pH. It can be associated to the potential competition between the H^+ and Hg^{2+} ions at acid pH. The higher affinity of H^+ toward the active sites of adsorption under low pH conditions during removal processes of different heavy metals has also been reported [38,39]. Additionally, the lower adsorption ability of Al-waste-NaP1 at acid pH could be related to the loss of active sites because of the partial dissolution of the zeolite. The influence of the pH on the crystallinity of the zeolite was also evaluated to select the most adequate conditions for the removal of all the heavy metals. It should be noted that the Al-waste-NaP1 zeolite presents a pH = 10 ± 0.5 when put in contact with aqueous solutions (due to its alkaline character derived from the zeolite synthesis process [11]). It was considered that acid pH could favor the adsorption of the metal cations. Fig. S4 compares the XRD patterns of the initial zeolite (Sample a) as well as those of the zeolite when it was put in contact with acid aqueous solutions for at least 1 h at pH 4 (Sample b), and pH 6 (Sample c). The results revealed that all samples exhibited well-defined XRD profiles showing the same zeolite phase typical of the NaP1 zeolite (reference file: ICDD PDF 01-071-0962). NaP1 zeolite is based on the gismondine-type framework and has a tetragonal crystal system. The most intense 301 reflection of Al-waste-NaP1 was centered at 28.07° (full width at half maximum, FWHM = 0.297°) for the Sample a, which showed a crystallite size of 24.8 nm. The variation of the solution pH seems to slightly modify the peak parameters and crystallite sizes of Al-waste-NaP1. Although the samples b and c also showed the 301 reflection centered at 28.08°, slight changes in the value of FWHM (0.368° and 0.341°) were found, leading to slightly smaller crystallite sizes (22.27 and 24.03 nm for samples b and c, respectively).

The mass of the zeolite remained unchanged for the pH range of 4–6. On the contrary, pH < 4 led to significant zeolite mass losses, between 48% and 86% for pH 3 and pH 2, respectively, as a consequence of the partial dissolution and dealumination of the zeolite [40]. Therefore, the solution pH should be controlled and kept constant in order to adequately evaluate the removal of the heavy metals by Al-waste-NaP1. Thus, the further removal experiments of the metal cations by Al-waste-NaP1 were performed at a fixed pH 4.5 to avoid zeolite mass losses caused by dissolution and dealumination and also to avoid the precipitation of the metal cations.

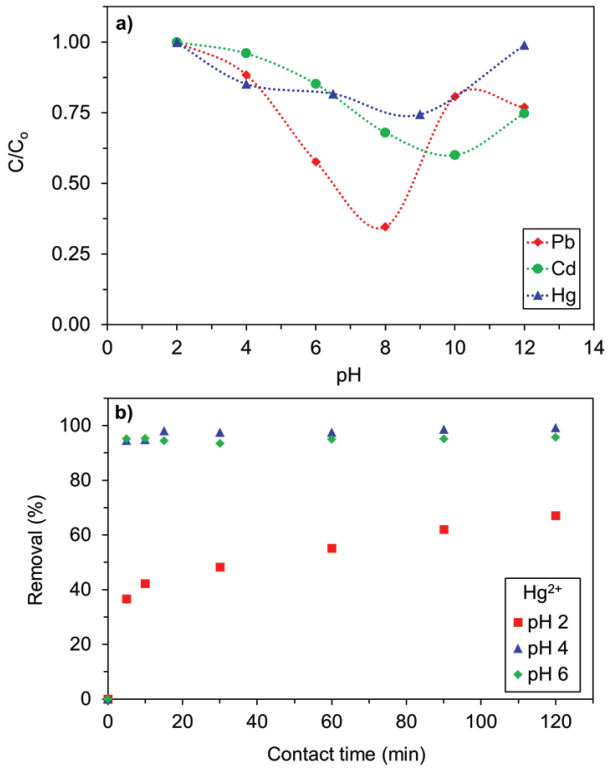

Fig. 1. (a) Effect of the solution pH on the stability of Pb^{2+}, Cd^{2+}, and Hg^{2+} in aqueous medium at 25°C ± 2. C/C_o: final concentration referred to the initial cation concentration (20 mg/L for Pb^{2+} and Cd^{2+}, and 0.2 mg/L for Hg^{2+}). (b) Influence of the solution pH on the removal efficiency of Hg^{2+} by Al-waste-NaP1. Conditions: zeolite dose = 10 g/L; C_o = 0.2 mg/L; T = 25 ± 2°C.

3.3. Effect of contact time: adsorption kinetics

The single-cation adsorption as a function of the contact time is shown in Fig. 2(a). As can be seen, the removal of each metal cation by Al-waste-NaP1 followed a very similar trend. The removal of Pb^{2+}, Cd^{2+}, and Hg^{2+} was a very fast process; the equilibrium was reached in less than 30 min, leading to high adsorption efficiencies (98.9%, 93.3%, and 99.3% for Pb^{2+}, Cd^{2+}, and Hg^{2+}, respectively, in 15 min). These results were related to the fast diffusion of the metal cations from the solution to the interface and to the zeolite structure which is accessible to the cations via its tridimensional channel system. The experiments were controlled up to 24 h in order to ensure no significant changes in the adsorption system. A contact time of 30 min was established as sufficient to achieve equilibrium conditions for all cations, leading to the following experimental removal capacities (q_t): 41.6, 3.8, and 0.045 mg/g for Pb^{2+}, Cd^{2+}, and Hg^{2+}, respectively. Figs. 2(b)–(d) depicts the pseudo-first-order and pseudo-second-order models for the removal of Pb^{2+}, Cd^{2+}, and Hg^{2+} by Al-waste-NaP1. The obtained kinetic parameters for each model are shown in Table 2. The results indicated that the pseudo-second-order model provided a significantly better correlation with the experimental data for the adsorption of all metal cations. Several studies also found that the pseudo-second-order model tends to describe satisfactorily the removal of diverse metals using sorbents from both chemicals and waste-based sources [41–43].

The Pb^{2+}, Cd^{2+}, and Hg^{2+} uptake by Al-waste-NaP1 was also evaluated by applying the intra-particle diffusion model (Table S2 and Fig. S5) in order to determine the rate-limiting steps of the adsorption. As the trendlines of the representation

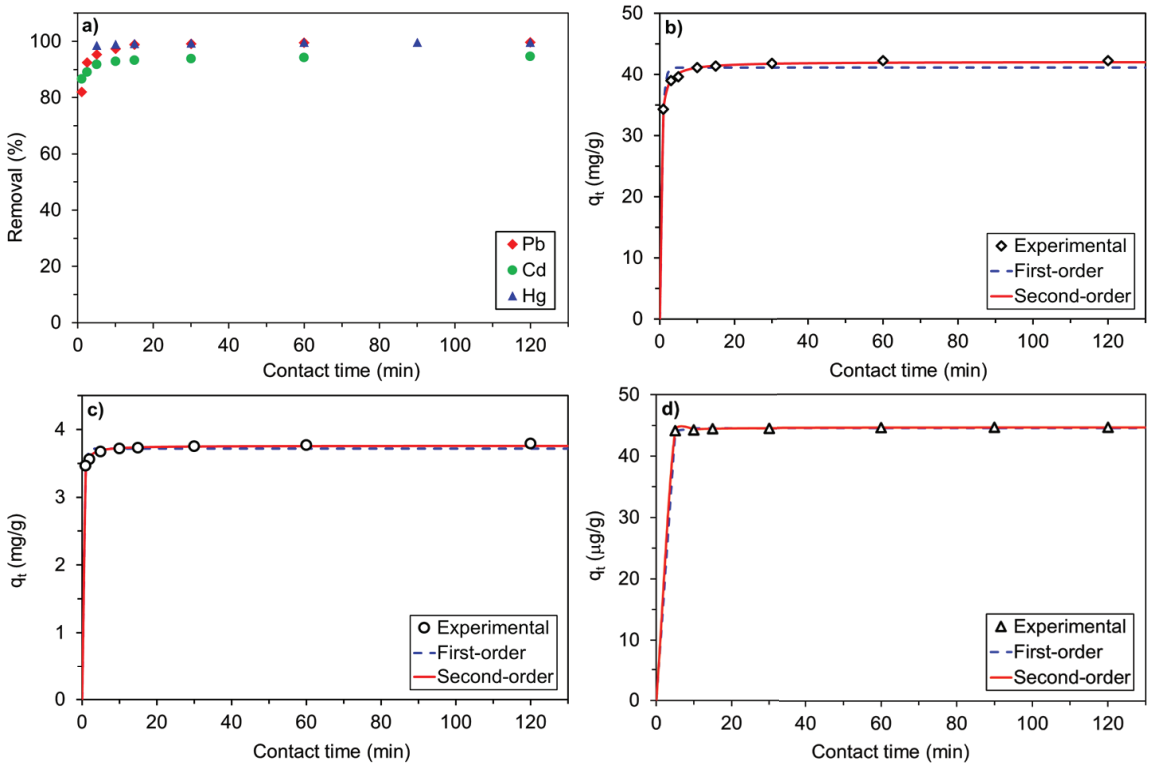

Fig. 2. Effect of the (a) contact time and pseudo-first-order and pseudo-second-order models for the single-cation adsorption of (b) Pb^{2+}, (c) Cd^{2+}, and (d) Hg^{2+} onto Al-waste-NaP1. Conditions: pH = 4.5; adsorbent dose = 5 g/L for Cd^{2+} and Hg^{2+}, and 0.5 g/L for Pb^{2+}; C_o = 20 mg/L for Pb^{2+} and Cd^{2+}, and 0.2 mg/L for Hg^{2+}; T = 25 ± 2°C.

plots did not pass through the origin, it means that the intra-particle diffusion was not the only rate-controlling step [20]. Thus, the overall adsorption process could be explained by a combination of fast bulk transport followed by film and intra-particle diffusion.

3.4. Effect of adsorbent dose

The influence of the solid–liquid ratio (i.e., ratio of zeolite mass referred to solution volume) or adsorbent dose for each metal cation was studied. Fig. 3 shows the effect of the adsorbent dose on the Pb^{2+}, Cd^{2+}, and Hg^{2+} adsorption efficiency and capacity of the zeolite. The metal cations adsorption efficiency increased along with the solid–liquid ratio or dose. In this sense, an increase in the mass of zeolite leads to an increase of the active sites on the adsorbent surface, thus favoring the adsorption process. Thus, Pb^{2+}, Cd^{2+}, and Hg^{2+} would diffuse from the aqueous solution toward the surface of Al-waste-NaP1, tending to occupy the available adsorption sites. The increase of adsorbent dose, involving larger amounts of zeolite available for the adsorbates, led to the decrease in the adsorption capacity of the metal cations. The elimination of the Pb^{2+} cation (Fig. 3(a)) involved the smallest doses of the zeolite, ranged between 0.125 and 1 g/L, compared with the Cd^{2+} and Hg^{2+} uptake (Figs. 3(b) and (c)) under the tested operating conditions. The results indicated that the adsorption ability of Al-waste-NaP1 seems to remain practically constant from an intermediate amount of zeolite, particularly for the Pb^{2+} and Cd^{2+} cations. Thus, an adsorbent dose of 0.5 g/L was fixed for the further Pb^{2+} removal experiments, while doses of 5 g/L were selected for both the Cd^{2+} and Hg^{2+} uptake.

Table 2
Kinetic model parameters and error function values calculated for the single adsorption of the Pb^{2+}, Cd^{2+}, and Hg^{2+} cations onto Al-waste-NaP1

Kinetic model	Parameters	Pb^{2+}	Cd^{2+}	Hg^{2+}
Pseudo-first order	$q_{t,\text{model}}$ (mg/g)	41.10	3.72	0.0445
$q_t = q_e\left(1 - e^{k_1 t}\right)$	k_1 (1/min)	1.77	2.61	0.96
	R^2	0.819	0.668	0.568
Pseudo-second order	$q_{t,\text{model}}$ (mg/g)	42.09	3.76	0.0446
$q_t = \frac{k_2 q_e^2 t}{1 + k_2 q_e t}$	k_2 (g/mg min)	0.10	2.86	0.38
	R^2	0.988	0.964	0.945
Experimental data	$q_{t,\text{experimental}}$ (mg/g)	42.27	3.79	0.0446

3.5. Effect of initial adsorbate concentration: equilibrium isotherms

The effect of the initial concentration of each metal cation on the adsorption capacity of Al-waste-NaP1 was evaluated applying the best conditions. The two-parameter and three-parameter isotherms and their derived parameters for each metal cation are shown in Fig. 4 and Table 3.

The amount of Pb^{2+}, Cd^{2+}, and Hg^{2+} removed by the zeolite increased progressively as the initial concentration of each heavy metal increased. The experimental data were

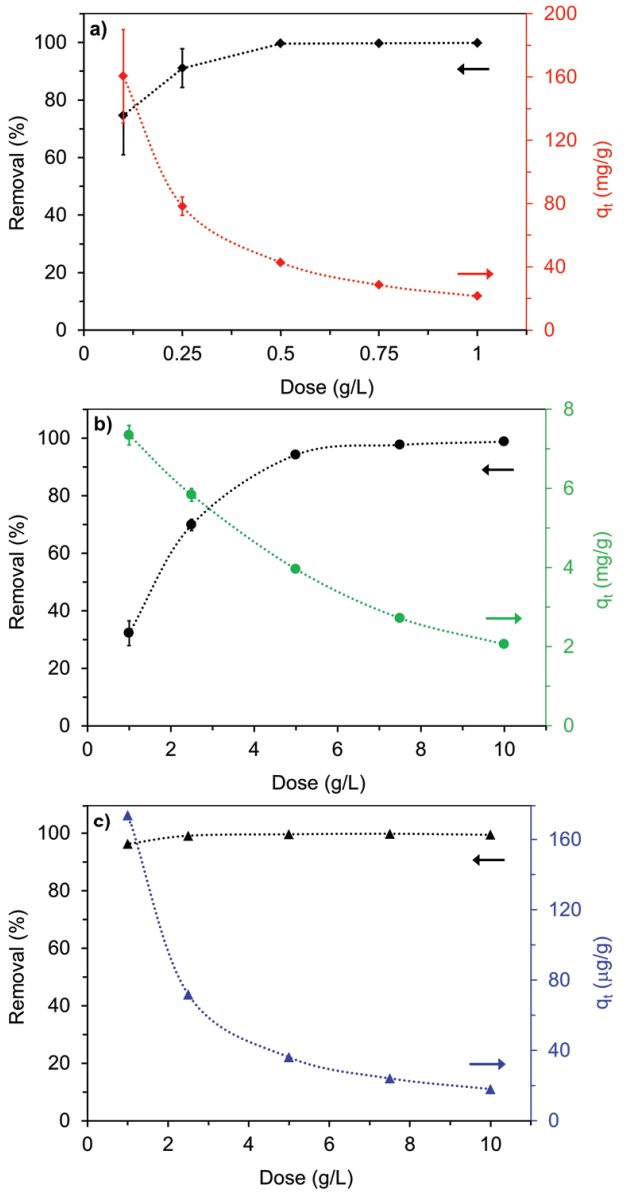

Fig. 3. Effect of the zeolite dose on the single-cation adsorption efficiency and uptake capacity of (a) Pb^{2+}, (b) Cd^{2+}, and (c) Hg^{2+} onto Al-waste-NaP1. Conditions: pH = 4.5; contact time = 30 min; C_o = 20 mg/L for Pb^{2+} and Cd^{2+}, and 0.2 mg/L for Hg^{2+}; T = 25 ± 2°C.

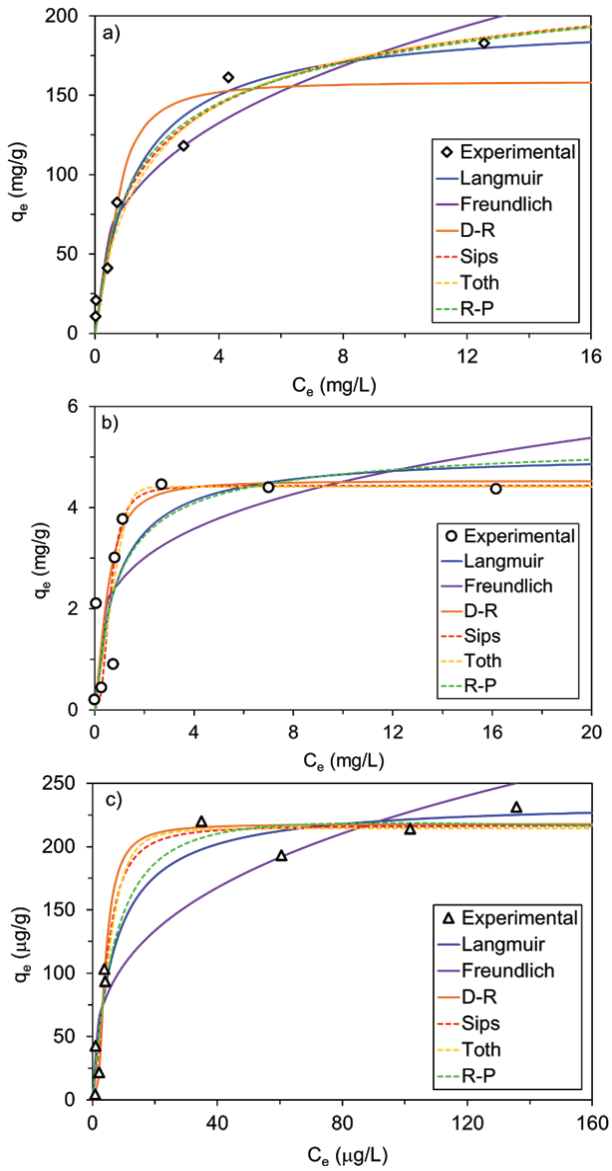

Fig. 4. Isotherms for the removal of (a) Pb^{2+}, (b) Cd^{2+}, and (c) Hg^{2+} on Al-waste-NaP1. Conditions: pH = 4.5; contact time = 15 min; adsorbent dose = 5 g/L for Cd^{2+} and Hg^{2+}, and 0.5 g/L for Pb^{2+}; T = 25 ± 2°C.

better described by the isotherm models based on three parameters. In particular, the Sips and Toth models provided the highest R^2 values. The experimental maximum removal capacity of the zeolite was 183, 4.37, and 0.23 mg/g for Pb^{2+}, Cd^{2+}, and Hg^{2+}, respectively. The maximum adsorption capacities obtained from the Sips isotherm model were 245.75, 4.43, and 0.22 mg/g for Pb^{2+}, Cd^{2+}, and Hg^{2+}, respectively. The Langmuir isotherm was the only two-parameter model that provided a good fit to the data in the whole range of initial concentrations. The nature of the adsorption process can be described through the Langmuir separation factor ($R_L = \frac{1}{1+k_L C_o}$), indicating if the adsorption is irreversible (R_L = 0), favorable (0 < R_L < 1), or unfavorable (R_L > 1) [44].

The experimental data led to R_L ranged 0.93–0.99, 0.96–0.99, and 0.84–0.99 for Pb^{2+}, Cd^{2+}, and Hg^{2+}, respectively. So, the removal of the metal cations using Al-waste-NaP1 could be explained by homogeneous adsorption on the active sites of the zeolite. In addition, the estimation of the sorption energy (1.9, 2.3, and 0.5 kJ/mol for Pb^{2+}, Cd^{2+}, and Hg^{2+}, respectively) using the Dubinin–Radushkevich model, revealed values of E < 8 kJ/mol, indicating that the metal cations uptake by Al-waste-NaP1 could take place by physical adsorption [6].

3.6. Competitive adsorption

The study of multi-cation adsorption allows for the assessment of the degree of interference of other metal cations present in the adsorption process. In this sense, the competitive

Table 3
Isotherm models: parameters and error function values obtained for the removal of the Pb^{2+}, Cd^{2+}, and Hg^{2+} cations onto Al-waste-NaP1

Isotherm	Parameters	Pb^{2+}	Cd^{2+}	Hg^{2+}
Two-parameter isotherm model				
Langmuir	q_{max} (mg/g)	198.18	5.08	0.24
$q_e = \frac{q_{max} k_L C_e}{1 + k_L C_e}$	k_L (L/mg)	0.78	1.11	1.47×10^{-4}
	R^2	0.967	0.819	0.954
Freundlich	k_F (mg/g)/(mg/L)^n	82.15	2.52	50.19
$q_e = k_F C_e^n$	n	0.35	0.25	0.33
	R^2	0.950	0.680	0.870
Dubinin–Radushkevich	q_{max} (mg/g)	158.55	4.53	0.22
$q_e = q_{DR} e^{-k_{DR}\varepsilon^2}$	k_{DR} (mol^2/kJ^2)	1.36×10^{-7}	9.23×10^{-8}	2.37×10^{-6}
	R^2	0.926	0.792	0.958
Three-parameter isotherm model				
Sips	q_{max} (mg/g)	245.75	4.43	0.22
$q_e = \frac{q_{max} (k_S C_e)^n}{1 + (k_S C_e)^n}$	k_S (L/mg)	0.41	1.62	2.23×10^{-4}
	n	0.70	2.81	1.83
	R^2	0.975	0.997	0.966
Toth	q_{max} (mg/g)	233.13	4.41	0.22
$q_e = \frac{q_{max} k_T C_e}{\left[1 + (k_T C_e)^n\right]^{1/n}}$	k_T (L/mg)	0.76	0.74	0.11
	n	0.75	6.97	3.0
	R^2	0.977	0.986	0.965
Redlich–Peterson	k_{RP} (L/g)	211.29	6.01	30.93
$q_e = \frac{k_{RP} C_e}{1 + a_{RP} C_e^{\beta}}$	a_{RP} (mg/L)$^{-\beta}$	1.41	1.27	9.09×10^{-5}
	β	0.89	0.97	1.08
	R^2	0.971	0.810	0.957

adsorption was evaluated using zeolite doses of 2 and 10 g/L at different contact times (ranged between 1 and 30 min), as shown in Table 4 and Fig. 5. It seems that Al-waste-NaP1 presented a greater affinity for Pb^{2+} compared with Cd^{2+} and Hg^{2+}. The multi-component removal efficiency of Pb^{2+} on the zeolite remained practically unchanged in presence of Hg^{2+} and Cd^{2+} under the studied conditions. High removal efficiencies of Pb^{2+} (almost 100 %) were reached both at very low contact times (1 min) and at longer times (i.e., 30 min), as can be seen in Fig. 5. In all the studied cases, the residual concentration of Pb^{2+} from both the single solution and the cations mixture was remarkably low (in both cases lower than 0.02 mg/L). The Cd^{2+} and Hg^{2+} removal efficiencies, which were lower than that obtained for Pb^{2+}, greatly increased in proportion to the zeolite dose. To evaluate the removal of Cd^{2+} and Hg^{2+} on the zeolite, the initial concentration of Pb^{2+} was varied (0–20 mg/L) using the best adsorption conditions (i.e., zeolite dose = 10 g/L; contact time = 30 min). In absence of Pb^{2+} in the solution medium, the elimination of such metal cations led to removal efficiencies ranged between 80% and 90 %. As the initial concentration of Pb^{2+} was increased, the Cd^{2+} and Hg^{2+} removal efficiencies were decreased due to the competition of the cations. From the results, the selectivity of Al-waste-NaP1 seems to follow the next sequence: $Pb^{2+} > Hg^{2+} \sim Cd^{2+}$, which is quite similar to that reported for heavy metals removal on natural zeolites [45]. Structurally, the zeolite presents eight-ring pore apertures, large enough for the accessibility of the metal cations through its channel system.

Table 4
Competitive adsorption of Pb^{2+}, Cd^{2+}, and Hg^{2+} on Al-waste-NaP1 using different zeolite doses and contact times

Cation	Adsorbent dose (g/L)	Contact time (min)	$q_{t,experimental}$ (mg/g)	Removal (%)
Pb^{2+}	2	5	10.47	98.8
		30	10.57	99.7
	10	5	2.15	99.9
		30	2.15	99.9
Cd^{2+}	2	5	2.15	20.3
		30	3.53	33.3
	10	5	1.83	85.1
		30	1.88	87.4
Hg^{2+}	2	5	0.042	42.2
		30	0.043	43.2
	10	5	0.018	86.0
		30	0.019	86.9

Conditions: pH = 4.5; C_o = 20 mg/L for Pb^{2+} and Cd^{2+}, and 0.2 mg/L for Hg^{2+}; T = 25 ± 2°C.

The hydrated radii of the studied metal cations are 0.401, 0.422, and 0.426 nm for Pb^{2+}, Hg^{2+}, and Cd^{2+}, respectively. So, the highest affinity of the zeolite for Pb^{2+} could be attributed to its smallest size that allows it to diffuse more easily to the zeolite surface.

3.7. Removal mechanism

For a better understanding of the adsorption mechanism between the adsorbent and metal cations, SEM, FTIR, and μ-XRF analysis were developed to study the morphological, structural, and chemical properties of the zeolite before and after the competitive adsorption. After the Pb^{2+}, Cd^{2+}, and Hg^{2+} removal, Al-waste-NaP1 exhibited the typical morphology of the initial zeolite [11] that remained unchanged (Fig. 6). Thus, the adsorption process of Pb^{2+}, Cd^{2+}, and Hg^{2+} at a pH 4.5 seems not to modify the zeolite structure. In addition, no precipitation of the studied heavy metals on the zeolite surface was observed in the SEM analysis. The comparison between the FTIR spectra of the initial zeolite with that obtained after the uptake of all the metal cations is shown in Fig. 7. Before the adsorption, the results show the typical absorption bands of the initial zeolite [11].

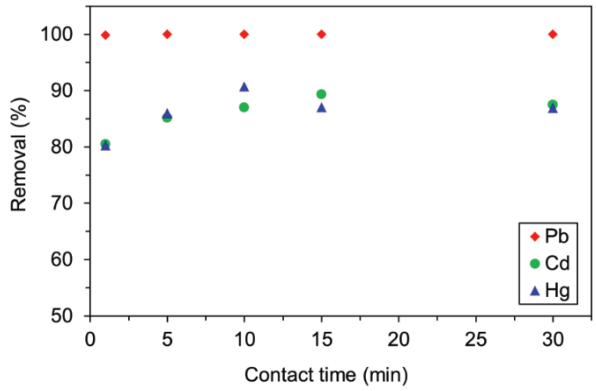

Fig. 5. Influence of the contact time on the multi-cation adsorption using Al-waste-NaP1. Conditions: pH = 4.5; adsorbent dose = 10 g/L; C_o = 20 mg/L for Pb^{2+} and Cd^{2+}, and 0.2 mg/L for Hg^{2+}; T = 25 ± 2°C.

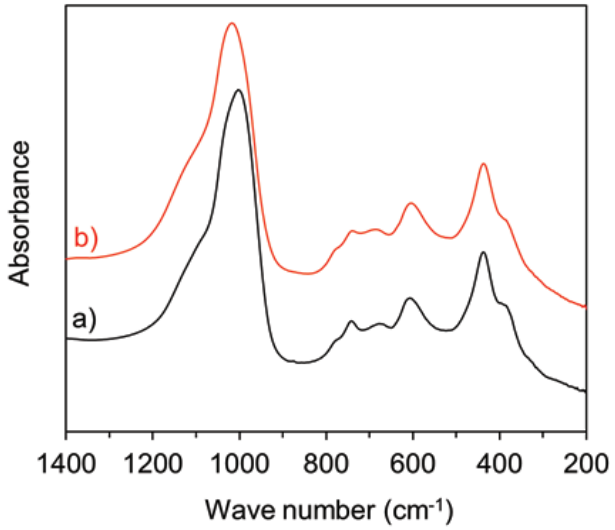

Fig. 7. FTIR spectra of Al-waste-NaP1 (a) before and (b) after the multi-cation adsorption of Pb^{2+}, Cd^{2+}, and Hg^{2+}.

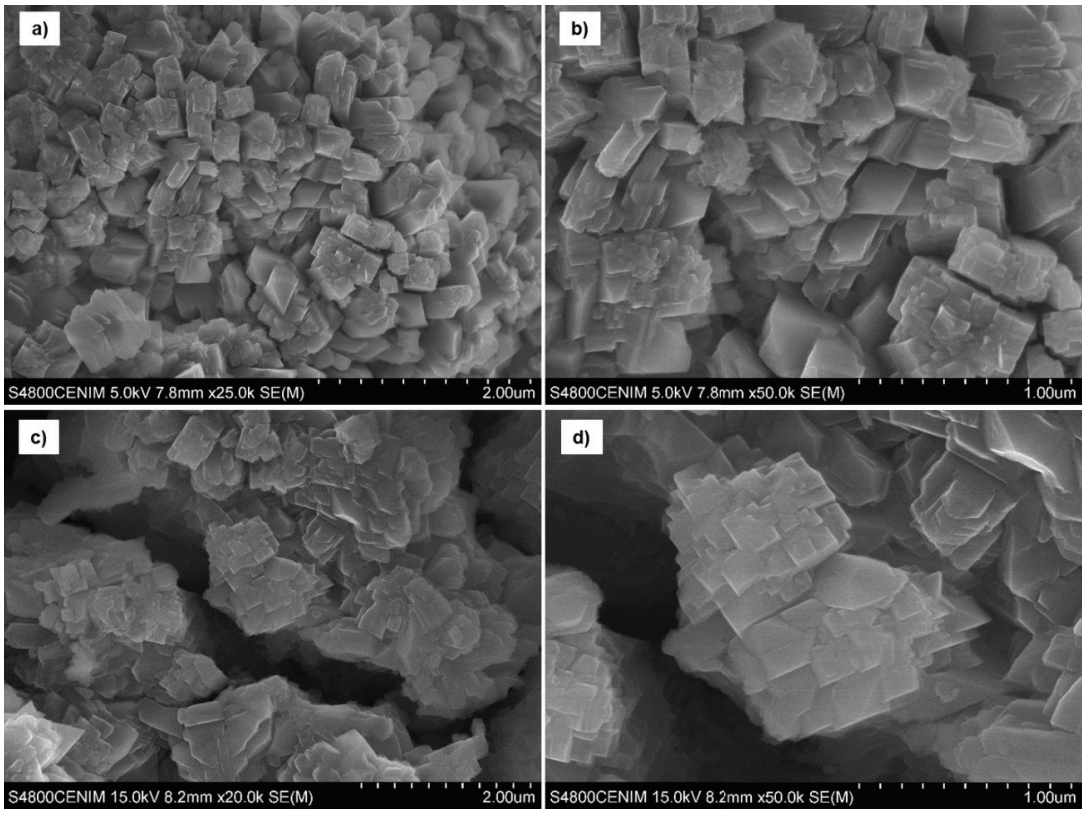

Fig. 6. SEM images of the Al-waste-NaP1 zeolite (a,b) before and (c,d) after the multi-cation removal of Pb^{2+}, Cd^{2+}, and Hg^{2+} from aqueous solutions.

The Pb^{2+}, Cd^{2+}, and Hg^{2+} adsorption seems to lead to very similar absorption bands to the characteristic vibration modes occurring in the initial zeolite. However, a slightly displacement of the bands associated to the T-O-T (T-atom: Si, Al) asymmetric (1,003 cm^{-1}) and symmetric (678 cm^{-1}) stretching modes of the initial zeolite was observed. After the adsorption, these absorption bands were shifted to 1,017 and 686 cm^{-1}, which is attributed to the uptake of the studied cations on Al-waste-NaP1. The reviewed literature reports changes in absorption bands that can be related to sorption processes of different contaminants from waters. For example, Mozgawa et al. [46] reported slight modifications in the intensity of absorption bands, around 650–715 cm^{-1}, of natural zeolites after the sorption of heavy metals. Zhu et al. [37] found shifts of bands to higher wave numbers that can be related to the coordination of metal cations with active groups on the sorbent. According to the Lewis acid–base theory, metal cations such as Pb^{2+}, Cd^{2+}, and Hg^{2+} could act as Lewis acids, while the active sites of the zeolite (mainly OH^-) could be considered as Lewis bases. Thus, the metal cations could react with OH^- on the zeolite surface by bonding to one or more available electron pairs on the base. To further understand the uptake of the Pb^{2+}, Cd^{2+}, and Hg^{2+} on Al-waste-NaP1, μ-XRF analysis was also performed to evaluate possible changes in the chemical composition of the zeolite before and after the multi-cation adsorption. The chemical composition (expressed as % wt.) of Al-waste-NaP1 after adsorption, compared with the initial zeolite, are shown in Table 5. Thus, the main chemical composition of Al-waste-NaP1 was as follows: SiO_2 55.16 wt.%, Al_2O_3 26.74 wt.%, Na_2O 7.62 wt.%, and ca 10 wt.% corresponding to small amounts of CaO, TiO_2, K_2O, Fe_2O_3, and MgO. As can be seen, both lead and cadmium were detected in the chemical composition of Al-waste-NaP1 after adsorption, confirming their immobilization on the zeolite. Mercury identification was not possible, as its residual concentration was below the detection limit of the XRF technique. This is probably due to its lower initial concentration used for adsorption tests. The amount of Na^+ present in the initial zeolite decreased as the heavy metals adsorption process progressed. This seems to indicate that the adsorption process could involve cation exchange between the extra-framework cations on the zeolite (mainly Na^+) and Pb^{2+}, Cd^{2+}, and Hg^{2+} through the mechanism represented in Fig. S6. These results are in accordance with those obtained by Meng et al. [47]. The authors studied the removal of cations including heavy metals such as Ag^+, Pb^{2+}, etc. onto a zeolite A from halloysite, reporting higher concentrations of Na^+ in the aqueous solution after adsorption.

Table 5
Chemical composition (determined by μ-XRF) of Al-waste-NaP1 before and after the competitive adsorption of Pb^{2+}, Cd^{2+}, and Hg^{2+}

Element	Before adsorption, % wt.	After adsorption, % wt.
SiO_2	55.16	57.16
Al_2O_3	26.74	27.17
Na_2O	7.62	3.75
CaO	2.88	2.75
TiO_2	2.77	3.01
K_2O	2.02	2.23
Fe_2O_3	1.18	1.15
MgO	0.96	0.55
ZnO	0.41	0.49
CuO	0.26	0.29
PbO	–	0.86
CdO	–	0.61

3.8. Comparison of the maximum adsorption capacity of Pb^{2+}, Cd^{2+}, and Hg^{2+} using different sorbent materials

Table 6 shows some sorbents used for the removal of the studied heavy metals from aqueous solutions compared with Al-waste-NaP1. The reviewed literature includes different sorbent materials (natural zeolites, clays, glasses, resins, nanocomposites, etc.) with different adsorption capacities, depending on the different experimental conditions studied (pH, temperature, adsorbent dose, contact time, cation initial concentration, etc.). As can be observed the adsorption capacity for Pb^{2+} of the Al-waste-NaP1 zeolite studied in this work is higher than those reported for the same cation, reaching it in a very short contact time.

4. Conclusions

The removal of Pb^{2+}, Cd^{2+}, and Hg^{2+} from synthetic aqueous solutions using an NaP1 zeolite synthesized from a hazardous aluminum waste was evaluated. The influence of the contact time on the single-cation removal followed a very similar trend for all the metal cations, reaching adsorption equilibrium in less than 30 min. The single-cation adsorption achieved high removal efficiencies: 98.9, 93.3, and 99.3% for Pb^{2+}, Cd^{2+}, and Hg^{2+}, respectively, in the first 15 min of the process. The pseudo-second-order kinetic model provided better correlation with the experimental data for all the adsorbates. The experimental data were best described by the Sips and Toth models. The experimental maximum removal capacity of the zeolite was 183, 4.37, and 0.23 mg/g for Pb^{2+}, Cd^{2+}, and Hg^{2+}, respectively. The maximum adsorption capacities obtained from the Sips isotherm model were 245.75, 4.43, and 0.22 mg/g for Pb^{2+}, Cd^{2+}, and Hg^{2+}, respectively. The removal of the metal cations could take place through a homogeneous and physical adsorption process. The studied zeolite presented the greatest affinity for Pb^{2+} compared with Cd^{2+} and Hg^{2+}. The multi-cation removal efficiency of Pb^{2+} remained practically unchanged in presence of Hg^{2+} and Cd^{2+}, reaching high removal efficiencies (almost 100%) both at very low contact times (1 min) and at longer times (30 min). The competitive adsorption followed a cation exchange mechanism between the extra-framework cations (mainly Na^+) and the Pb^{2+}, Cd^{2+}, and Hg^{2+} cations.

Accordingly, this work implies a synergic effect on the environmental protection: firstly, the transformation of the hazardous aluminum waste into a zeolite can contribute to its end-of-waste condition, and secondly, the zeolite obtained from such waste can be considered as a promising adsorbent used for the treatment of aqueous effluents contaminated by endocrine disruptors.

Table 6
Comparison of the maximum adsorption capacity of Pb^{2+}, Cd^{2+}, and Hg^{2+} using different sorbent materials

Adsorbent	q_{max} (mg/g)	Isotherm	pH	Dose (g/L)	Time (h)	T (°C)	Ref.
Lead (Pb^{2+}) removal							
Ti(IV) iodovanadate	18.8	Langmuir	6	2	1	20	[48]
Bentonite	19.5	Freundlich	6	2	24	RT	[39]
Ethylene diamine tetra acetic acid-Zr(IV) iodate	26.0	Langmuir	6	10	0.83	25	[49]
Clinoptilolite	40.7	Sips	5	2	72	30	[15]
Polyaniline supported nanocomposite	44.6	Freundlich	6	2	1	20	[50]
NaP1 from oil shale ash	70.6	R–P	7	1	5	20	[51]
Fig sawdust	80.7	Langmuir	4	1.7	0.83	25	[52]
Erionite	81.3	Sips	5	2	72	30	[15]
Modified natural zeolite	133	Freundlich	4.2	20	24	RT	[53]
Al-waste-NaP1	245.8	Sips	4.5	0.5	0.5	25	This work
Fe nanoparticles loaded ash	833.3	Langmuir	6	1	0.7	25	[54]
Cadmium (Cd2+) removal							
Clinoptilolite	2.5	Sips	5	2	72	30	[15]
Al-waste-NaP1	4.4	Sips	4.5	5	0.5	25	This work
Erionite	4.6	Sips	5	2	72	30	[15]
Bentonite	13.1	Freundlich	6	2	24	RT	[39]
NaP1 from oil shale ash	95.6	Sips	7	1	5	20	[51]
Curcumin formaldehyde resin	119.1	Langmuir	7	1	1	25	[55]
Mercury (Hg2+) removal							
Al-waste-NaP1	0.22	Sips	4.5	5	0.5	25	This work
Perlite	0.35	Langmuir	6.5	14	1.33	20	[56]
Bentonite	1.7	Freundlich	6	10	36	RT	[39]
Organosilica	5.4	–	4.5	0.01	0.5	21	[57]
Ti(IV) iodovanadate	17.2	Langmuir	6	2	1.5	20	[48]
Polyaniline-Zr (IV) phosphoborate	154	Langmuir	6	0.4	3	25	[58]
Starch/SnO2	192	Langmuir	6	0.4	1	25	[59]
Modified amberlite resin	270	Langmuir	6	1	1.5	25	[60]
NiFe2O4-bearing nitrogen-doped mesoporous carbon	476	Langmuir	6	4	2	25	[61]

Acknowledgments

The authors thank MINECO for its financial support (Project CTM2012-34449). R. Sánchez-Hernández thanks MINECO for the grant BES-2013-066269. The authors also thank the Centre of Research Support of the Geology Faculty of University Complutense of Madrid for the help given.

References

[1] M. Ferrante, G.O. Conti, Z. Rasic-Milutinovic, D. Jovanovic, Health Effects of Metals and Related Substances in Drinking Water, IWA Publishing, London, UK, 2013.
[2] Minamata Convention on Mercury: Text and Annexes, United Nations Environment Programme, Geneva, Switzerland, 2013.
[3] K. Tanong, L. Coudert, G. Mercier, J.-F. Blais, Recovery of metals from a mixture of various spent batteries by a hydrometallurgical process, J. Environ. Manage., 181 (2016) 95–107.
[4] Directive 2013/39/EU of the European Parliament and of the Council of 12 August 2013 Amending Directives 2000/60/EC and 2008/105/EC as Regards Priority Substances in the Field of Water Policy, O.J., L 226 (2013) 1–17.
[5] P.-S. Keng, S.-L. Lee, S.-T. Ha, Y.-T. Hung, S.-T. Ong, Removal of hazardous heavy metals from aqueous environment by low-cost adsorption materials, Environ. Chem. Lett., 12 (2014) 15–25.
[6] R. Apiratikul, P. Pavasant, Sorption of Cu^{2+}, Cd^{2+}, and Pb^{2+} using modified zeolite from coal fly ash, Chem. Eng. J., 144 (2008) 245–258.
[7] Y.J.O. Asencios, M.R. Sun-Kou, Synthesis of high-surface-area γ-Al_2O_3 from aluminum scrap and its use for the adsorption of metals: Pb (II), Cd (II) and Zn (II), Appl. Surf. Sci., 258 (2012) 10002–10011.
[8] Y. Zhou, S. Xia, J. Zhang, Z. Zhang, S.W. Hermanowicz, Adsorption characterizations of biosorbent extracted from waste activated sludge for Pb (II) and Zn (II), Desal. Wat. Treat., 57 (2016) 9343–9353.
[9] R. Sánchez-Hernández, A. López-Delgado, I. Padilla, R. Galindo, S. López-Andrés, One-step synthesis of NaP1, SOD and ANA from a hazardous aluminum solid waste, Microporous Mesoporous Mater., 226 (2016) 267–277.
[10] R. Galindo, I. Padilla, O. Rodríguez, R. Sánchez-Hernández, S. López-Andrés, A. López-Delgado, Characterization of solid wastes from aluminum tertiary sector: the current state of Spanish industry, J. Mineral. Mater. Charact. Eng., 3 (2015) 55.
[11] R. Sánchez-Hernández, I. Padilla, S. López-Andrés, A. López-Delgado, Eco-friendly bench-scale zeolitization of

an Al-containing waste into gismondine-type zeolite under effluent recycling, J. Cleaner Prod., 161 (2017) 792–802.
[12] Directive 2008/98/EC of the European Parliament and of the Council of 19 November 2008 on waste and repealing certain Directives (Text with EEA relevance), O.J., L 312, 2008, pp. 3–30.
[13] X. Kong, Z. Han, W. Zhang, L. Song, H. Li, Synthesis of zeolite-supported microscale zero-valent iron for the removal of Cr^{6+} and Cd^{2+} from aqueous solution, J. Environ. Manage., 169 (2016) 84–90.
[14] C. Li, H. Zhong, S. Wang, J. Xue, Z. Zhang, A novel conversion process for waste residue: synthesis of zeolite from electrolytic manganese residue and its application to the removal of heavy metals, Colloids Surf., A, 470 (2015) 258–267.
[15] V. Hernández-Montoya, M.A. Pérez-Cruz, D.I. Mendoza-Castillo, M.R. Moreno-Virgen, A. Bonilla-Petriciolet, Competitive adsorption of dyes and heavy metals on zeolitic structures, J. Environ. Manage., 116 (2013) 213–221.
[16] P. Barragán, M.G. Macedo, M.T. Olguín, Cadmium sorption by sodium and thiourea-modified zeolite-rich tuffs, J. Environ. Sci., 52 (2017) 39–48.
[17] S.Y. Lagergren, Zur Theorie der sogenannten Adsorption gelöster Stoffe, K. Sven. Vetenskakad. handl., 24 (1898) 1–39.
[18] G. Blanchard, M. Maunaye, G. Martin, Removal of heavy metals from waters by means of natural zeolites, Water Res., 18 (1984) 1501–1507.
[19] W.J. Weber, J.C. Morris, Kinetics of adsorption on carbon from solution, J. Sanit. Eng. Div., 89 (1963) 31–60.
[20] H.N. Tran, S.-J. You, A. Hosseini-Bandegharaei, H.-P. Chao, Mistakes and inconsistencies regarding adsorption of contaminants from aqueous solutions: a critical review, Water Res., 120 (2017) 88–116.
[21] I. Langmuir, The adsorption of gases on plane surfaces of glass, mica and platinum, J. Am. Chem. Soc., 40 (1918) 1361–1403.
[22] H.M.F. Freundlich, Over the adsorption in solution, J. Phys. Chem., 57 (1906) 385–471.
[23] M.M. Dubinin, L.V. Radushkevich, Equation of the characteristic curve of activated charcoal, Proc. Acad. Sci. Phys. Chem. Section., 55 (1947) 331–333.
[24] O. Redlich, D.L. Peterson, A useful adsorption isotherm, J. Phys. Chem., 63 (1959) 1024–1024.
[25] J. Toth, State equations of the solid-gas interface layers, Acta Chim. Acad. Sci. Hung., 69 (1971) 311–328.
[26] R. Sips, On the structure of a catalyst surface, J. Chem. Phys., 16 (1948) 490–495.
[27] O. Larlus, S. Mintova, T. Bein, Environmental syntheses of nanosized zeolites with high yield and monomodal particle size distribution, Microporous Mesoporous Mater., 96 (2006) 405–412.
[28] S. Vallar, D. Houivet, J. El Fallah, D. Kervadec, J.M. Haussonne, Oxide slurries stability and powders dispersion: optimization with zeta potential and rheological measurements, J. Eur. Ceram. Soc., 19 (1999) 1017–1021.
[29] P. Scherrer, Estimation of the size and internal structure of colloidal particles by means of röntgen, Nachr. Ges. Wiss. Göttingen, 2 (1918) 96–100.
[30] G. Gillies, R. Raj, F.-D. Kopinke, A. Georgi, Suspension stability and mobility of Trap-Ox Fe-zeolites for in-situ nanoremediation, J. Colloid Interface Sci., 501 (2017) 311–320.
[31] M. Kosmulski, IEP as a parameter characterizing the pH-dependent surface charging of materials other than metal oxides, Adv. Colloid Interface Sci., 171–172 (2012) 77–86.
[32] N. Arancibia-Miranda, S.E. Baltazar, A. García, D. Muñoz-Lira, P. Sepúlveda, M.A. Rubio, D. Altbir, Nanoscale zero valent supported by zeolite and montmorillonite: template effect of the removal of lead ion from an aqueous solution, J. Hazard. Mater., 301 (2016) 371–380.
[33] M.R. Das, J.M. Borah, W. Kunz, B.W. Ninham, S. Mahiuddin, Ion specificity of the zeta potential of α-alumina, and of the adsorption of p-hydroxybenzoate at the α-alumina-water interface, J. Colloid Interface Sci., 344 (2010) 482–491.
[34] J.A. Menendez, M.J. Illán-Gómez, C.A. León y León, L.R. Radovic, On the difference between the isoelectric point and the point of zero charge of carbons, Carbon, 33 (1995) 1655–1657.
[35] Y. Zhou, S. Xia, J. Zhang, B.T. Nguyen, Z. Zhang, Insight into the influences of pH value on Pb (II) removal by the biopolymer extracted from activated sludge, Chem. Eng. J., 308 (2017) 1098–1104.
[36] D. Datta, H. Uslu, Adsorptive separation of lead (Pb^{2+}) from aqueous solution using tri-n-octylamine supported montmorillonite, J. Chem. Eng. Data, 62 (2017) 370–375.
[37] M. Zhu, L. Zhu, J. Wang, T. Yue, R. Li, Z. Li, Adsorption of Cd (II) and Pb (II) by in situ oxidized Fe_3O_4 membrane grafted on 316L porous stainless steel filter tube and its potential application for drinking water treatment, J. Environ. Manage., 196 (2017) 127–136.
[38] Y. Yan, Q. Li, X. Sun, Z. Ren, F. He, Y. Wang, L. Wang, Recycling flue gas desulphurization (FGD) gypsum for removal of Pb (II) and Cd (II) from wastewater, J. Colloid Interface Sci., 457 (2015) 86–95.
[39] Y. Fernández-Nava, M. Ulmanu, I. Anger, E. Marañón, L. Castrillón, Use of granular bentonite in the removal of mercury (II), cadmium (II) and lead (II) from aqueous solutions, Water Air Soil Pollut., 215 (2011) 239–249.
[40] C.S. Cundy, P.A. Cox, The hydrothermal synthesis of zeolites: precursors, intermediates and reaction mechanism, Microporous Mesoporous Mater., 82 (2005) 1–78.
[41] X. Li, C. Bian, X. Meng, F.-S. Xiao, Design and synthesis of an efficient nanoporous adsorbent for Hg^{2+} and Pb^{2+} ions in water, J. Mater. Chem. A, 4 (2016) 5999–6005.
[42] A. Gil, S. Albeniz, S.A. Korili, Valorization of the saline slags generated during secondary aluminium melting processes as adsorbents for the removal of heavy metal ions from aqueous solutions, Chem. Eng. J., 251 (2014) 43–50.
[43] R.R.Z. Tarpani, F.R. Lapolli, M.Á. Lobo-Recio, Removal of aluminum from synthetic solutions and well water by chitin: batch and continuous experiments, Desal. Wat. Treat., 53 (2015) 3531–3542.
[44] E. Worch, Adsorption Technology in Water Treatment: Fundamentals, Processes, and Modeling, Walter de Gruyter, Germany, 2012.
[45] S. Wang, Y. Peng, Natural zeolites as effective adsorbents in water and wastewater treatment, Chem. Eng. J., 156 (2010) 11–24.
[46] W. Mozgawa, M. Król, T. Bajda, Application of IR spectra in the studies of heavy metal cations immobilization on natural sorbents, J. Mol. Struct., 924–926 (2009) 427–433.
[47] Q. Meng, H. Chen, J. Lin, Z. Lin, J. Sun, Zeolite A synthesized from alkaline assisted pre-activated halloysite for efficient heavy metal removal in polluted river water and industrial wastewater, J. Environ. Sci., 56 (2017) 254–262.
[48] M. Naushad, Z.A. ALOthman, M.R. Awual, M.M. Alam, G.E. Eldesoky, Adsorption kinetics, isotherms, and thermodynamic studies for the adsorption of Pb^{2+} and Hg^{2+} metal ions from aqueous medium using Ti (IV) iodovanadate cation exchanger, Ionics, 21 (2015) 2237–2245.
[49] M. Naushad, Z.A. Alothman, Inamuddin, H. Javadian, Removal of Pb (II) from aqueous solution using ethylene diamine tetra acetic acid-Zr (IV) iodate composite cation exchanger: kinetics, isotherms and thermodynamic studies, J. Ind. Eng. Chem., 25 (2015) 35–41.
[50] R. Bushra, M. Naushad, R. Adnan, Z.A. Alothman, M. Rafatullah, Polyaniline supported nanocomposite cation exchanger: synthesis, characterization and applications for the efficient removal of Pb^{2+} ion from aqueous medium, J. Ind. Eng. Chem., 21 (2015) 1112–1118.
[51] R. Shawabkeh, A. Al-Harahsheh, M. Hami, A. Khlaifat, Conversion of oil shale ash into zeolite for cadmium and lead removal from wastewater, Fuel, 83 (2004) 981–985.
[52] M. Ghasemi, M. Naushad, N. Ghasemi, Y. Khosravi-fard, A novel agricultural waste based adsorbent for the removal of Pb (II) from aqueous solution: kinetics, equilibrium and thermodynamic studies, J. Ind. Eng. Chem., 20 (2014) 454–461.
[53] M. Kragović, A. Daković, Ž. Sekulić, M. Trgo, M. Ugrina, J. Perić, G.D. Gatta, Removal of lead from aqueous solutions by using the natural and Fe (III)-modified zeolite, Appl. Surf. Sci., 258 (2012) 3667–3673.

[54] M. Ghasemi, M. Naushad, N. Ghasemi, Y. Khosravi-fard, Adsorption of Pb (II) from aqueous solution using new adsorbents prepared from agricultural waste: adsorption isotherm and kinetic studies, J. Ind. Eng. Chem., 20 (2014) 2193–2199.
[55] M. Naushad, T. Ahamad, Z.A. Alothman, M.A. Shar, N.S. AlHokbany, S.M. Alshehri, Synthesis, characterization and application of curcumin formaldehyde resin for the removal of Cd^{2+} from wastewater: kinetics, isotherms and thermodynamic studies, J. Ind. Eng. Chem., 29 (2015) 78–86.
[56] H. Ghassabzadeh, A. Mohadespour, M. Torab-Mostaedi, P. Zaheri, M.G. Maragheh, H. Taheri, Adsorption of Ag, Cu and Hg from aqueous solutions using expanded perlite, J. Hazard. Mater., 177 (2010) 950–955.
[57] M.A.O. Lourenço, P. Figueira, E. Pereira, J.R.B. Gomes, C.B. Lopes, P. Ferreira, Simple, mono and bifunctional periodic mesoporous organosilicas for removal of priority hazardous substances from water: the case of mercury(II), Chem. Eng. J., 322 (2017) 263–274.
[58] R. Bushra, M. Naushad, G. Sharma, A. Azam, Z.A. ALOthman, Synthesis of polyaniline based composite material and its analytical applications for the removal of highly toxic Hg^{2+} metal ion: antibacterial activity against *E. coli*, Korean J. Chem. Eng., 34 (2017) 1970–1979.
[59] M. Naushad, T. Ahamad, G. Sharma, A.a.H. Al-Muhtaseb, A.B. Albadarin, M.M. Alam, Z.A. Alothman, S.M. Alshehri, A.A. Ghfar, Synthesis and characterization of a new starch/SnO_2 nanocomposite for efficient adsorption of toxic Hg^{2+} metal ion, Chem. Eng. J., 300 (2016) 306–316.
[60] M. Naushad, S. Vasudevan, G. Sharma, A. Kumar, Z.A. Alothman, Adsorption kinetics, isotherms, and thermodynamic studies for Hg^{2+} adsorption from aqueous medium using alizarin red-S-loaded amberlite IRA-400 resin, Desal. Wat. Treat., 57 (2016) 18551–18559.
[61] M. Naushad, T. Ahamad, B.M. Al-Maswari, A. Abdullah Alqadami, S.M. Alshehri, Nickel ferrite bearing nitrogen-doped mesoporous carbon as efficient adsorbent for the removal of highly toxic metal ion from aqueous medium, Chem. Eng. J., 330 (2017) 1351–1360.

Supplementary

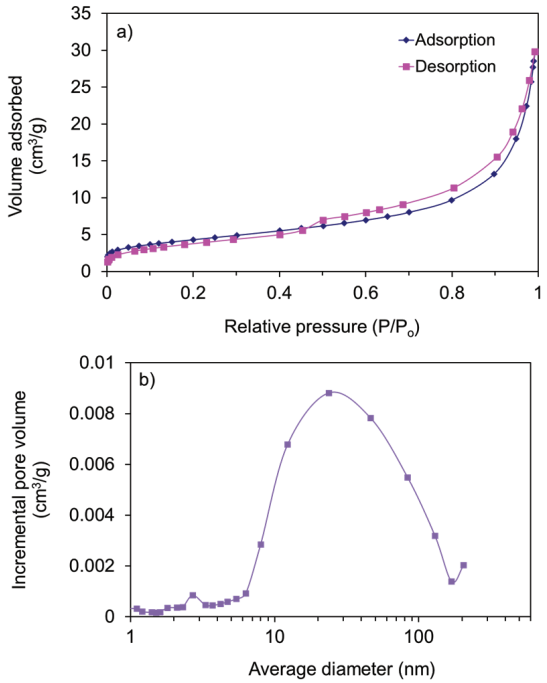

Fig. S1. Nitrogen adsorption/desorption isotherm (Type IV) and pore size distribution of Al-waste-NaP1.

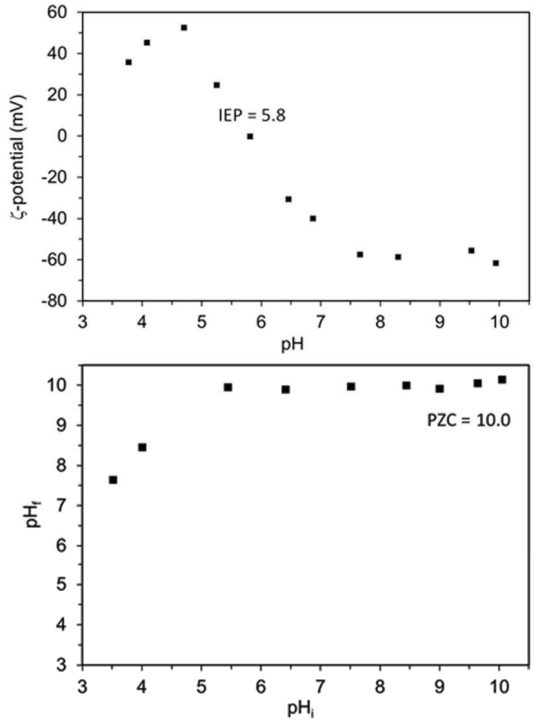

Fig. S2. ζ-potential and PZC of Al-waste-NaP1 in aqueous solution at 25°C.

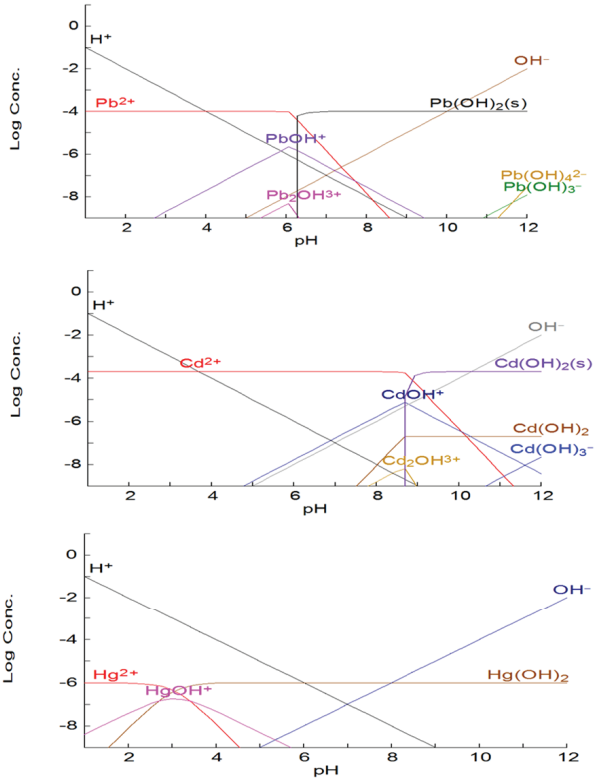

Fig. S3. Chemical equilibrium diagrams of Pb^{2+}, Cd^{2+}, and Hg^{2+} in aqueous solution determined for the following initial concentrations: 20 mg/L for Pb^{2+} and Cd^{2+}, and 0.2 mg/L for Hg^{2+}.

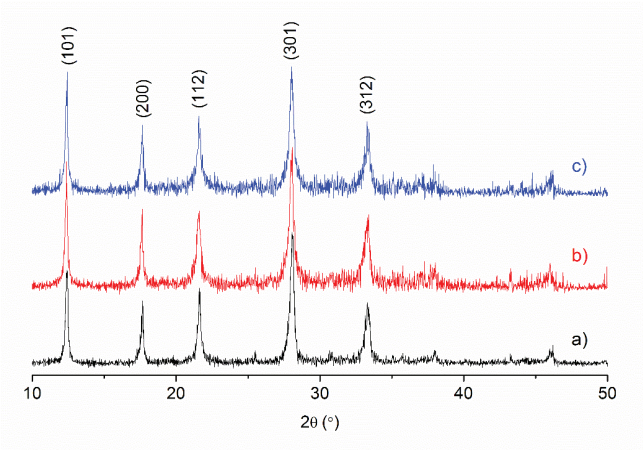

Fig. S4. Comparison of the XRD patterns of the zeolite at different pH values: (a) initial sample of zeolite (Al-waste-NaP1) at pH 10 ± 0.5; (b) samples of zeolite in aqueous solutions at pH 4, and (c) at pH 6. In all the cases, NaP1-type zeolite was identified according to the reference file: ICDD PDF 01-071-0962.

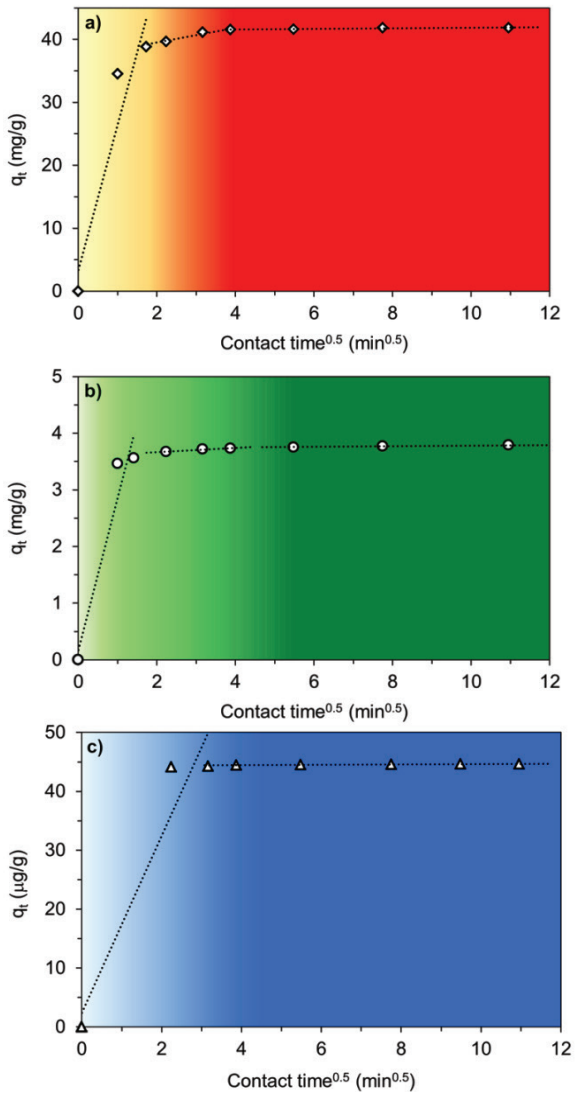

Fig. S5. Intra-particle diffusion models of the adsorption of (a) Pb^{2+}, (b) Cd^{2+}, and (c) Hg^{2+} onto Al-waste-NaP1. Conditions: pH = 4.5; adsorbent dose = 5 g/L for Cd^{2+} and Hg^{2+}, and 0.5 g/L for Pb^{2+}; C_o = 20 mg/L for Pb^{2+} and Cd^{2+}, and 0.2 mg/L for Hg^{2+}; T = 25 ± 2°C.

Table S1
Cation exchange capacity (CEC) and textural properties of Al-waste-NaP1

CEC (meq/g)	S_{BET} [a] (m^2/g)	S_{EXT} [b] (m^2/g)	V_{total} [c] (cm^3/g)	V_{micro} [d] (cm^3/g)	V_{meso} [e] (cm^3/g)	D_p [f] (nm)
2.4	15.17	14.43	0.04559	0.00038	0.04521	12.16

[a]BET-specific surface area was obtained from N_2 adsorption isotherm in the relative pressure range of 0.003–0.3.
[b]External area was calculated from the *t*-plot method.
[c]Total pore volume was estimated for the N_2 amount adsorbed at the relative pressure of 0.99.
[d]Micropore volume was calculated from the *t*-plot method.
[e]Mesopore volume was calculated as the difference between V_{total} and V_{micro}.
[f]Average pore diameter was estimated, assuming cylindrical pore shape, from the next equation: $D_p = 4V/S_{BET}$.

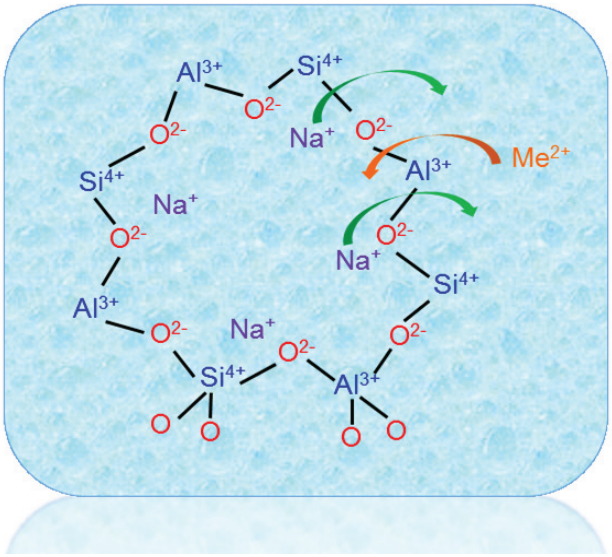

Fig. S6. Adsorption mechanism based on cation exchange between the extra-framework cations (Na^+) of the Al-waste-NaP1 zeolite and the heavy metal cations (Pb^{2+}, Cd^{2+}, and Hg^{2+}, represented as Me^{2+}).

Table S2
Parameters obtained from the intra-particle diffusion model applied to the adsorption of Pb^{2+}, Cd^{2+}, and Hg^{2+} using Al-waste-NaP1

Cation	Step	Intra-particle diffusion model $q_t = k_p t^{0.5} + C$		
		k_p (mg/g min$^{0.5}$)	C (mg/g)	R^2
Pb^{2+}	1	5.18	29.43	0.99
	2	1.11	37.60	0.99
	3	0.046	41.38	0.73
Cd^{2+}	1	0.160	3.31	0.98
	2	0.015	3.67	0.99
	3	0.004	3.74	0.93
Hg^{2+}	1	$1.78 \cdot 10^{-4}$	$4.38 \cdot 10^{-2}$	0.99
	2	$3.30 \cdot 10^{-5}$	$4.43 \cdot 10^{-2}$	0.94